IRIS AperTO

UNIVERSITÀ DEGLI STUDI DI TORINO

AperTO - Archivio Istituzionale Open Access dell'Università di Torino

The influence of surface charge and photo-reactivity on skin-permeation enhancer property of nano-TiO2 in ex vivo pig skin model under indoor light

This is the author's manuscript

Original Citation:

Availability:

This version is available http://hdl.handle.net/2318/155488 since 2016-07-21T11:20:00Z

Published version:

DOI:10.1016/j.ijpharm.2014.03.052

Terms of use:

Open Access

Anyone can freely access the full text of works made available as "Open Access". Works made available under a Creative Commons license can be used according to the terms and conditions of said license. Use of all other works requires consent of the right holder (author or publisher) if not exempted from copyright protection by the applicable law.

(Article begins on next page)

25 December 2024

UNIVERSITÀ DEGLI STUDI DI TORINO

This Accepted Author Manuscript (AAM) is copyrighted and published by Elsevier. It is posted here by agreement between Elsevier and the University of Turin. Changes resulting from the publishing process - such as editing, corrections, structural formatting, and other quality control mechanisms - may not be reflected in this version of the text. The definitive version of the text was subsequently published in INTERNATIONAL JOURNAL OF PHARMACEUTICS, 467, 2014, 10.1016/j.ijpharm.2014.03.052.

You may download, copy and otherwise use the AAM for non-commercial purposes provided that your license is limited by the following restrictions:

(1) You may use this AAM for non-commercial purposes only under the terms of the CC-BY-NC-ND license.

(2) The integrity of the work and identification of the author, copyright owner, and publisher must be preserved in any copy.

(3) You must attribute this AAM in the following format: Creative Commons BY-NC-ND license (http://creativecommons.org/licenses/by-nc-nd/4.0/deed.en), 10.1016/j.ijpharm.2014.03.052

The definitive version is available at:
http://linkinghub.elsevier.com/retrieve/pii/S0378517314002075

The Influence of Surface Charge and Photo-reactivity on Skin-Permeation Enhancer Property of Nano-TiO_2 in Ex-Vivo Pig Skin Model Under Indoor Light

Elena Peira[a,*], Francesco Turci[b,c,*], Ingrid Corazzari[b,c], Daniela Chirio[a], Luigi Battaglia[a], Bice Fubini[b,c], Marina Gallarate[a]

[a] Dip. Scienza e Tecnologia del Farmaco, University of Torino, via P. Giuria 9, 10125, Torino, Italy

[b] Dip. Chimica, University of Torino, via P. Giuria 7, 10125,Torino, Italy

[c] "G. Scansetti" Interdepartmental Center and NIS Excellence Center, via P. Giuria 9, 10125,Torino, Italy

*Corresponding authors:

Dr. Elena Peira

e-mail: elena.peira@unito.it

Phone: +39 011 6707668 / Fax: +39 011 670 7687

Dip. Scienza e Tecnologia del Farmaco, University of Torino, via P. Giuria 9, 10125, Torino, Italy

Dr. Francesco Turci

e-mail: francesco.turci@unito.it

Phone: +39 011 6707577 / Fax: +39 011 670 7855

Dip. Chimica, University of Torino, via P. Giuria 7, 10125,Torino, Italy

Abstract

Several topical products contain nanometric TiO_2 (nano-TiO_2), which is an useful and safe component that absorbs UV light and does not cross skin barrier. However nano-TiO_2 may impregnate the first layer of the skin (stratum corneum, SC) and generate free radicals, even under low UV irradiation. These properties, largely dependent on TiO_2 surface chemistry, may modulate the transdermal drug permeation. To investigate how TiO_2 surface properties affect drug permeation, Amphotericin in two different media, in the presence of three differently coated samples, was applied on skin and the flux measured. The naked, but not the coated, nano-TiO_2 showed enhancer property, with a fourfold increase of the drug flux. Only the positively–charged naked TiO_2 strongly adhered to and altered the SC structure. The oxidative potential towards formate anion and linoleic acid was assessed and a molecular mechanism to elucidate increased skin permeability proposed. To enhance the drug permeation, both a surface charge-driven adhesion and an oxidative disorganization of the SC lipids are required. By modulating TiO_2 surface charge (coating) and its oxidative potential (crystalline phase), the enhancer effect of nano-TiO_2 may be tuned and turned up or down when transdermal penetration of drug has to be favored or impaired.

Keywords: nanometric TiO_2, drug permeation, skin-permeation enhancer, pig skin, oxidative potential, free radical

Chemical compounds studied in this article

Titanium dioxide (PubChem CID: 26042); Amphotericin B (PubChem CID: 5280965)

1. Introduction

In the cosmetic field, titanium dioxide (TiO_2) has traditionally been used in sunscreen lotions because of its properties of ultraviolet A (UVA) and B (UVB) light absorption/scattering and its cosmetic acceptability (Serpone et al., 2007). TiO_2 is also widely used as a pharmaceutical excipient and it is described in the European Pharmacopoeia.

TiO_2 is available in three different crystalline forms: rutile, anatase, and brookite, in addition to an amorphous phase. Only rutile and anatase have relevance in pharmaceutical and cosmetic field (Mitsui, 1997). The main difference between the two crystalline forms is the divergence in photo-activity, with anatase being the most photoactive form of titanium dioxide (Diebold, 2003). In contrast, rutile is the most common form of titania (Silva and Faria, 2009). It has been also reported that a combination of anatase and rutile exhibits enhanced photocatalytic features (Bolis et al., 2012). In the presence of UV light, TiO_2 is activated to produce reactive oxygen species such as hydroxyl radicals, superoxide anions and singlet oxygen (Daimon et al., 2008). Indeed, the risk of damage to DNA and RNA, caused by the photocatalytic effect of nano-TiO_2 after absorption of UV light, can be prevented by particles coating with organic and inorganic materials (Serpone et al., 2007). They are expected to reduce the oxide photo-reactivity (Carlotti et al., 2009), and, mostly in the case of silane-coated TiO_2, to enhance the compatibility with the lipophilic ingredients of the cosmetic preparations.

In recent years, manufacturers have started using the nanosized form of TiO_2 in place of its bulk form. Using nanosized particles generates products with improved texture and more vibrant color. Sunscreen formulations with nanosized forms of TiO_2 have resolved the problem of the unsightly white film of traditional sunscreens and created a vehicle that is more transparent, less viscous and blends into the skin more easily (Newman et al., 2009). However the introduction of TiO_2 ultrafine particles has raised the question of whether the particles used in TiO_2-based cosmetic products have the potential to penetrate through the stratum corneum (SC) into viable skin layers via intercellular

channels, hair follicles and sweat glands (Menzel et al., 2004). The intercellular space between the cells composing the SC is approximately 100 nm^3 and may be widened with topical application of various products (Baroli, 2010). Therefore, nano-TiO_2 is suspected to pass through it. Several authors have studied the possible penetration of nano-TiO_2 into the skin, using both naked and coated titania samples (Bennat and Muller-Goymann, 2000; Dussert et al., 1997; Gamer et al., 2006; Pflucker et al., 2001 and Schulz et al., 2002). Generally TiO_2, also nanometric, does not penetrate the skin nor the underlying living tissue, remaining on the skin surface or only impregnating the first layers of SC.

The tight SC structure and molecular composition prevent the entrance of active substances and therapeutic agents and therefore the diffusion across the SC, the non-living outer layer of the skin, is normally impaired (Elias, 2005; Lee et al., 2006). Diffusion across the SC is hence the rate-limiting step for percutaneous absorption of many drugs (Padula et al., 2011). One long-standing approach to increase the range of drugs that can be effectively delivered via this route is the use of penetration enhancers, which interact with the skin to reversibly decrease the barrier resistance and to promote the drug flux (Williams and Barry, 2004).

As a consequence of such ability to impregnate the first layers of SC as well as to form complexes with proteins and to induce the formation of free radicals (Borm et al., 2006; Turci et al., 2013; Carlotti et al., 2009, 2007; Fenoglio et al., 2013, 2011), nano-TiO_2 could increase transdermal permeation of drugs or active ingredients, when used as an excipient in pharmaceutical products or as UV filter in sunscreen lotions.

This study is aimed to investigate the effect of surface chemistry on the possible enhancing effect elicited by nano-TiO_2 on the transdermal permeation of drugs. A naked and two differently coated, commercially available, nano-TiO_2 were chosen and their surface properties (surface charge, surface area, and particle size distribution) assessed. Amphotericin B (AmB), an antifungal agent, that, owing to a bulky structure, does not easily permeate the skin (Dollery et al., 1991), was used as model drug in the permeation studies. The AmB flux was estimated by delivering on the skin the

drug mixed with the differently coated nano-TiO_2 in two different media. The molecular determinants of the TiO_2-skin interaction were examined by evaluating i) the surface feature driving adhesion to skin and ii) the chemical reaction taking place during the interaction. The strength of the adhesion with SC of nano-TiO_2 was assessed *ex vivo* by means of micro X-ray fluorescent chemiometric imaging (μ-XRF) performed on washed cross-section of skin. Raman spectroscopy and differential scanning calorimetry (DSC) of the SC were also carried out and the structural changes induced in the skin determined. The oxidative potential of the three differently coated nano-TiO_2 was investigated in a in vitro cell-free system by assessing i) the radical reactivity towards formate ion, as a probe of potential rupture of a C–H bond, with the spin-trapping technique, and ii) the potency to peroxidate lipids by measuring in vitro the degradation of linoleic acid. The interaction between nano-TiO_2 and skin was described at the molecular level and possible both positive and negative outcomes envisaged.

2. Experimental

2.1 TiO_2 nano-powders.

One naked and two variously coated, commercially available, TiO_2-based nanomaterials (nano-TiO_2) have been employed. Aeroxide P25 (naked nano-TiO_2) and Tego Sun TS plus (trimethoxycaprylylsilane and amorphous silica coated nano-TiO_2) were kindly gifted by Evonik (Essen, Germany). PW Covasil S-1 (trimethoxycaprylylsilane coated nano-TiO_2) was kindly gifted by LCM Trading S.p.A. (Sesto San Giovanni, Italy).

The crystal structure of the TiO_2 core was checked by Raman spectroscopy (see Supporting Information, Figure S-1).

Amorphous silica nano-powder (Aerosil 50, from Evonik, Essen, Germany) was used as negative control in some experiments.

2.2 Chemicals

All chemicals, whereas not differently stated, were from Sigma-Aldrich (Milan, Italy). Tegosoft EE (octyl octanoate) was supplied from A.c.e.f. (Fiorenzuola d'Adda, Piacenza, Italy), glycerol from Labochem and Amphotericin B (AmB) from Fluka. Phytocream 2000 (Potassium Palmitoyl Hydrolyzed Wheat Protein, Glyceryl stearate, Cetearyl Alcohol) was from Sinerga s.r.l., dimethyl sulfoxide (DMSO) from Merck. For all the aqueous solutions ultrapure milli-Q water (Millipore, Billerica, MA) was employed.

2.3 Nanoparticle characterization

2.3.1. Mean diameter and ζ potential determination of nano-TiO_2

Nano-TiO_2 was characterized by mean diameter and polydispersity measurements employing the dynamic light scattering technique-DLS (90 Plus Particle Size Analyzer, Brookhaven Instruments Corporation, NewYork, USA) at the fixed angle of 90°. All the samples were suspended in DMSO aqueous solutions (10% v/v, without pH modification) and dispersed by a rod-shaped stirring magnetic bar for 60 min. Measurements were performed on appropriate diluted samples (1:100 with DMSO aqueous solution) to avoid multiple scattering.

ζ potential of TiO_2 samples was measured by electrophoretic measurements (Zeta potential) using the ZetaPlus-Zeta Potential Analyzer (Brookhaven Instruments Corporation, NewYork, USA). Measurements were carried out on TiO_2 samples in DMSO aqueous solution (10% v/v). To assess the real surface charge exhibited by TiO_2 samples during the skin-interaction experiments, ζ potential was measured without altering the pH of the dispersion medium.

Each system was analyzed three times and ten size determinations were done for each sample at 25 ± 0.1 °C.

2.3.2. Radical-driven surface reactivity

To assess the radical-driven reactivity of the TiO_2 samples, the generation of carbon-centered free radicals and lipoperoxidation of linoleic acid, chosen as a model of cell membrane fatty acid, were measured. All the experiments were carried out under controlled indoor illumination.

Generation of carbon-centered radical: 28 mg of TiO_2 samples were suspended in 0.5 ml of sodium formate (1 M) buffered solution (potassium phosphate buffer, 125 mM, pH 7.4) in the presence of DMPO (5,5-dimethyl-1-pyrroline-1-oxide, 75mM, Alexis Biochemicals, San Diego, CA) as spin-trapping agent. The powder suspension was continuously stirred and exposed to controlled indoor illumination during the experiment. The ESR spectra were recorded on 50 μL of the suspension withdrawn after 60 minutes. The experiment was repeated three times with similar results. Splitting constants of the signal recorded: $a^N = 1.56$ mT $a^H = 1.87$ mT.

In vitro lipoperoxidation (TBA assay): the potential of nano-TiO_2 to induce lipid peroxidation was assessed by means of thiobarbituric acid (TBA) assay using linoleic acid as a model of polyunsaturated fatty acids in the cell membrane. The main lipoperoxidation product malonyldialdheyde (MDA) forms with TBA a colored complex. The assay is based on the reactivity of MDA - a colorless molecule - with TBA to produce a pink adduct which absorbs at 535 nm. Nano-TiO_2 was suspended (15 mg/ml) in a buffered (5 mM, pH 7.4 potassium phosphate buffer) dispersion of linoleic acid (1 mM) containing 2.5 wt. % ethanol. The suspension was continuously stirred under controlled indoor illumination at room temperature for 72 h. The lipid peroxidation was stopped by adding 0.1 ml of an ethanolic solution of butyl hydroxyl toluene (BHT, 0.2 wt. %) to the suspension. The nano-TiO_2 was removed by centrifugation (20 000 × g for 30 min). A solution of TBA (0.034 M) containing HCl (0.25 M) and trichloroacetic acid (0.92 M) was added to the supernatant (2:1 v:v) and the resulting solution was heated at 100 °C for 1 h. After cooling in an ice bath, 3 ml 1-butanol were added to extract the colored complexes. The absorbance at 535 nm was measured on the organic phase by means of a UV/Vis spectrophotometer (Uvikon, Kontron Instruments, Inc., Everett, MA, USA). The experiments were repeated at least three times.

2.4 Controlled indoor illumination conditions

To simulate a best-case scenario, all experiments were carried out under controlled indoor illumination with a very low content of UV light. The light irradiance was measured by a portable photoradiometer (Deltahom, Caselle di Selvazzano, Padova, Italy) equipped with two detectors operating in the Vis−NIR range (400–1050 nm) and in the UVA range (315–400 nm). An irradiance of ca. 750 mW/m^2 (Vis-NIR range) and <1 mW/m^2 (UVA) was measured during all experiments. It is worth noting that experiments of TiO_2-induced photodegradation of skin are commonly carried out with an UVA irradiance >10 W/m^2 (simulating outdoor summer sunlight), about 10 000 times higher than our experimental settings.

2.5 Permeation studies of AmB through the porcine skin in the presence of nano-TiO_2

2.5.1 Preparation of AmB-containing oil-in-water (O/W) emulsion in presence of nano-TiO_2

A conventional O/W emulsion to spread the drug and the nano-TiO_2 on the skin was prepared. 14% w/v Tegosoft EE and 3% w/v Phytocream 2000 were melted and added to the warm glycerin aqueous solution (5%w/v) under continuous homogenization by a T25 Ultra-Turrax (IKA). AmB (0.2 mg/ml) was added to the emulsion kept to a temperature < 40 °C. The emulsion was stirred until room temperature was reached. Finally, TiO_2 was dispersed (5 mg/ml) in the emulsion under homogenization.

2.5.2 Preparation of AmB-containing DMSO aqueous solution in the presence of nano-TiO_2

A simplified dispersion medium was also prepared. AmB was dissolved in DMSO and water was added drop wise up to an aqueous dilution of DMSO to 10% v/v. Final AmB concentration was 2 mg/ml. The DMSO was added to dissolve the AmB. DMSO is a polar aprotic solvent with a skin permeation enhancer properties but it improves the permeation of a wide range of compounds at

concentrations exceeding 60% (Anigbogu et al., 1995). TiO_2 samples were suspended in this solution at 5 mg/ml.

2.5.3 Procedure of permeation studies

The permeation of drug from the formulations into (topical delivery) and through (transdermal delivery) porcine skin, used as a model membrane, was performed using vertical Franz-type diffusion cells (Franz, 1975).

Skin from the ear region was excised and then the subcutaneous fat and connective tissue were removed. The obtained skins were washed, visually examined for integrity, and then placed in a refrigerator at 4 °C overnight. Just before the experiments, full-thickness skin was rinsed with normal saline and pre-hydrated soaking the SC kept upward in 0.002% w/v aqueous sodium azide, to maintain an *in vivo* trans-epidermal hydration.

The skin was then sandwiched between two areas of round glass with the surface up. The formulations (500 µl) under study were accurately applied to the skin surface, which had an available permeation area of 1.7 cm^2. Test formulations were applied to three skins from each pig in a parallel experimental setup. Three skin preparations per pig were treated with the AmB formulations without TiO_2 to determine the permeation of drug in absence of the inorganic nanomaterials.

50% v/v ethanol was used as receiving medium to ensure sink conditions (AmB solubility 14 µg/ml) and continuously stirred at 35°C. At appropriate intervals, the receiving medium was collected and HPLC determination of AmB promptly performed. The cell was immediately refilled with fresh receiving medium.

At the end of the permeation experiment (24 h), the surface of the skin was washed with 50% v/v ethanol, rinsed with physiological saline solution and subjected to further analysis to assess the drug accumulated. The skin was cut into small pieces. The tissue was further homogenized with 10% v/v DMSO in methanol and left for 4 h at room temperature for extraction of drug from the skin. After

shaking for 15 minutes and centrifuging for 5 minutes at 5000 rpm, AmB content in porcine skin was analyzed by HPLC.

AmB flux was determined from the slope and intercept of the straight line obtained by plotting the amount of AmB in the receptor compartment versus time in steady state conditions.

2.6 AmB HPLC analysis

HPLC analysis of AmB was performed as reported by Wilkinson et al. (1998). The liquid chromatograph consisted of a pump (LC 10-AD), an UV-VIS detector (JASCO UV-1575), a data station (Shimadzu, Kyoto, Japan), and a RP-C18 column 250mm × 4.6mm, 5 μm (Symmetry Shield® Waters, Milford, MA). The mobile phase was methanol:acetonitrile:2.5 mM Na_2-EDTA in water (50:30:20 v/v/v) at a flow rate of 1.2 ml·min^{-1}. The injection volume was 20 μl and the monitoring wavelength 405 nm. Under these conditions AmB retention time is 4.36 min.

2.7 Interaction studies of nano-TiO_2 with pig skin

To understand how nano-TiO_2 interacts with the structures of the skin and eventually affects the permeation of AmB, the suspension containing nano-TiO_2 was contacted with full-thickness pig ear skin by using vertical Franz-type diffusion cells. A simplified dispersion medium was used and TiO_2 samples were suspended (5 mg/ml) in the 10 % DMSO aqueous solution, and applied to the donor site of the pig skin surface. An area of 1.7 cm^2 was available for diffusion.

The content of the receptor cell (6 ml water) was continuously stirred and thermostated at 35°C, under controlled indoor illumination (UVA <1 mW/m^2).

At the end of the experiments (24 h), skin surface was washed five times with 50% v/v ethanol, then with normal saline solution to remove excess nano-TiO_2. Skins were collected to perform DSC studies or micro-XRF and Raman confocal spectroscopy studies. To perform micro-XRF and Raman studies, skin samples were frozen and cut into 30-μm-thickslices in vertical sections with

the use of a cryomicrotome (CM1900, Leica Microsystem, Wetzlar, Germany) and transferred onto glass microscopy slides. Skin samples used for these studies were obtained without fixative media.

2.8 X-ray Fluorescence Spectroscopy (μ -XRF).

The presence of nano-TiO_2 on the skin was assessed by micro-XRF imaging. The washed thin cross sections of untreated and TiO_2-contacted skin were analyzed using an EDAX Eagle III energy-dispersive μ-XRF spectrometer equipped with a Rh X-ray tube and a polycapillary exciting a circular area of nominally 30 μm diameter. The Kα fluorescent line of Ti was integrated pixel by pixel with a lateral resolution of 32×25 pixel (0.155 pixel/μm). The final image resolution was further improved μm acquiring spectra from partially overlapping points. Each map was recorded using identical acquisition conditions (40 eV, 1000 μA, dwell time = 5000 msec) and the Ti Kα intensities plotted using a pseudo-color thermal scale (black = 0, white = 100 cps).

2.9 Micro-Raman spectroscopy

The conformational changes induced on lipids and proteins of the SC by TiO_2 have been followed investigating the symmetric and asymmetric vibrational stretching modes of CH, CH_2 and CH_3. The laser beam of a confocal Raman microscope (Horiba Jobin-Yvon HR800 and Olympus BX41 microscope) has been focused on a 1 μm×1 μm wide portion of the SC. A polarized solid state Nd laser operating at λ=532.11 nm and at 80 mW power and a CCD air-cooled detector operating at − 70°C were used. The use of visible laser beam (λ = 532 nm) as excitation source minimize the oxidative degradation of the skin samples possibly induced by the UV photoreactiviy of TiO_2. Calibration of the instruments was performed by measuring the Stokes and anti-Stokes bands of the Si band at 520.7 cm^{-1}. Samples were placed on a polished stainless steel slide and a 50 × objective delivering a power of c. 15 mW on the sample was used. Spectra were acquired with a spectral

resolution of ca. 2 cm^{-1} and an integration time spanning from 100 to 400 seconds. The absence of structural modification induced by the heat generated by the laser photon flux was evaluated recording and superimposing a time-resolved series of spectra collected from the same tissue spot. To increase the signal to noise ratio and take into account the intrinsic variability of biological tissue, at least 10 spectra per skin sample, collected from distinct portions of the SC, were recorded, baseline subtracted, and averaged. Since skin cross section density may vary from sample to sample, the Raman intensity of each spectrum was corrected by normalizing the intensity of the maximum at 2937 cm^{-1} to 1 arbitrary unit.

2.10 Differential scanning calorimetry (DSC)

DSC experiments were performed to study the interaction between the tested formulations and SC lipid structure. Thermal transition at 70-73°C, attributed to phase changes in the intercellular lipid bilayers (Al-Saidan et al., 1998) was followed. A Perkin Elmer differential calorimeter (DSC7, Perkin Elmer, Nortwalk, Conn. USA) equipped with an instrument controller Tac 7/DX (Perkin Elmer) was used. After 24h interaction studies the pig skin was washed five time with 50% v/v ethanol. The pig skin samples were treated as reported by Yamane et al. (1995) to part the stratum corneum from the other skin layers. The SC samples obtained were weighed (about 10 mg), hermetically encapsulated in stainless-steel pans and analyzed. A heating rate of 10 °C/min was employed in the 25-110 °C temperature range.

Data are reported as mean ± SD of at least three independent measures and relative variation of lipid transition enthalpy measured at ca. 70° C evaluated as follows:

$$\%\Delta H = (1 - \frac{\Delta H_{sample}}{\Delta H_{blank}}) \times 100$$

where ΔH_{sample} is the enthalpy measured on the skin contacted with nano-TiO_2 and ΔH_{blank} the lipid transition enthalpy measured on skin section, obtained from the same donor site, contacted with dispersion medium (untreated skin).

2.11 Data report

Each set of experiments was performed at least three times. Results are reported as means ± standard deviations (SD).

3. Results

3.1 Nano-TiO_2 characterization

The main characteristics and the physical-chemical properties of the studied samples, including crystal phase composition, primary particle size, type of coating and specific surface area, are reported in Table 1.

The three samples are made of mixed phases of anatase and rutile, in the 9:1 ratio, roughly estimated by Raman spectroscopy (see Supporting Information). Primary particle size of TiO_2 samples ranges from 10 to 50 nm. Because of the identical ratio of the two crystal phase, it is arguable that the three samples are made of the same anatase/rutile raw material and are differentiated only by the surface coating. The samples will be hereafter referred as AR (for anatase/rutile), followed by the type of coating, namely, none (AR), silane coated (AR-SL), and silane and silica coated (AR-SL-S).

Because nano-TiO_2 samples are prone to aggregate in aqueous media and this process is largely dependent on the particle surface charge, the size of aggregates/agglomerates, which may eventually form, and ζ potential in the DMSO aqueous solution was measured by means of DLS and ELS techniques, respectively. The nano-TiO_2 suspensions in O/W emulsion were not characterized, because O/W intrinsic opacity is not suitable for in situ DLS/ELS measurements. Other techniques (e.g., electron microscopies) or dilution would not reproduce the actual experimental conditions used to delivery nano-TiO_2 to the skin. In Table 1, the mean hydrodynamic diameter (d_H) of particle aggregates/agglomerates is reported. When nano-TiO_2 was dispersed in the delivery medium, the pH of the aqueous suspension becomes slightly acidic, namely 5.40, 6.00, and 6.02 for AR, AR-SL, and AR-SL-S, respectively. Under these experimental conditions, naked anatase/rutile ζ potentials values is +9.10 mV, whereas coated AR-SL and AR-SL-S are negatively charged, with a ζ potential of −17.1 mV and −20.7 mV respectively. Clearly, the occurrence of the coating influences the surface charge and depends on the chemical nature of the coating itself.

Naked AR has a point of zero charge of 6.1 pH units (see Supporting Information, Figure S-3), and is thus positively charged at pH lower than 6.1, while at similar pH values silane and silane-silica coated nano-TiO_2 are negatively charged. On its turn, surface charge likely influences particle aggregation in the dispersion medium. In fact, the uncoated AR shows a larger aggregate/agglomerate size of 266 nm, whereas the more electrically charged surface of AR-SL and AR-SL-S determines a better dispersion of the particles with an average hydrodynamic size of 190 and 207 nm, respectively. Particle size dispersion is reported as polydispersity index (PDI), also a parameter for DLS data quality.

3.2 TiO_2-induced enhancement of drug permeation

The model drug AmB was dissolved (0.2 mg/ml) in the DMSO aqueous solution containing 5 mg/ml of suspended nano-TiO_2, and was used in skin permeation studies. The same experiments were also carried out dissolving AmB and nano-TiO_2 in a more realistic oil/water delivery medium. The drug flux was measured as reported in 2.5.3 subsection and the flux ratio ($\Delta\Phi$) was calculated as:

$$\Delta\Phi = \frac{\Phi_{TiO_2} - \Phi_{Blank}}{\Phi_{Blank}}$$

where Φ_{TiO_2} is the AmB flux measured through the skin exposed to nano-TiO_2 suspension and Φ_{Blank} is the AmB flux in the absence of TiO_2. The Figure 1A illustrates the variation of AmB flux, induced by the occurrence of anatase/rutile (AR), silane-coated (AR-SL), and silane-silica coated (AR-SL-S) nano-TiO_2 samples on the skin. Experiments were performed dissolving the model drug in two media, differing for hydrophilicity, namely DMSO aqueous solution (light grey bars) and oil/water emulsion (dark grey). The data of flux ratio clearly indicate that naked nano-TiO_2 behaves as a permeation enhancer both when incorporated in DMSO aqueous solution and O/W emulsion.

At the opposite, silane and silane-silica coated nano-TiO_2 do not significantly increase the drug flux, when incorporated in both media.

The effect of the different coatings on drug skin accumulation was evaluated by quantifying the amount of AmB adsorbed on the skin section contacted with AR, AR-SL and AR-SL-S dispersed in both delivery media. The relative accumulation ratio ($\Delta\Theta$):

$$\Delta\Theta = \frac{\Theta_{TiO_2} - \Theta_{Blank}}{\Theta_{Blank}}$$

where Θ_{TiO_2} is the AmB amount measured in skin exposed to nano-TiO_2 suspension and Θ_{Blank} is the amount detected on skin not brought in contact with nano-TiO_2, is reported in Figure 1B. The graph gives evidence of the variation of AmB accumulation in the skin section, induced by naked (AR), silane-coated (AR-SL), and silane-silica coated (AR-SL-S) anatase/rutile nano-TiO_2. A very slight increase of accumulation was induced by naked AR delivered in O/W emulsion medium, while the presence of coated samples, delivered in both media, did not significantly alter the drug accumulation in skin. In the present case, naked nano-TiO_2 acts as potent penetration enhancer, but a negligible increase of accumulation is observed. The molecular understanding of this peculiar behavior is far beyond the purpose of this paper. The tight intercellular space in the SC efficiently limits the diffusion large molecules. When SC structure is altered and pores widened, the large molecules may be moved to viable skin layers. The accumulation of a drug in the different layers of the skin is the result of several factors, among which its affinity with the vehicle and the skin seems to be one of the most relevant.

[INSERT FIG1 HERE]

3.3 Nano-TiO_2 adhesion with the skin

The effect of surface coating on the reversibility of the nano-TiO_2 interaction with the skin was investigated by evaluating the strength of nanomaterial adhesion following washing procedure. The

adhesion was quantified by means of a μ-XRF spectroscope. Such technique allows direct visualization of unlabeled nano-TiO_2 in the ppm range, with a spatial resolution of few microns. Untreated and TiO_2-contacted skin were cross-sectioned and imaged integrating pixel by pixel the Si, Cl, and Ti Kα X-ray fluorescence lines, with a lateral resolution of 32×25 pixel. Figure 2 reports the light microscopy image of the thin skin cross sections (*a*), with the SC evidenced by an overlaid dotted line, and the elemental colorimetric mapping of the same area, integrated for the ROI intensity of Si, Cl, and Ti fluorescence peaks (*b*, *c*, and *d* panel, respectively). Images from untreated (DMSO aqueous solution) skin sections (A) and skin exposed to naked AR in the same medium (B) are reported. The pseudocolor images of Si, from the glass slide supporting the section, and Cl, from the isotonic solution used to wash the skin after drug diffusion experiment, allowed us to reconstruct the profile of skin sections and to point out discontinuity in section density (chlorine map, panel *c*). The occurrence of Ti throughout the SC was similarly highlighted (panel *d*). In all cases, TiO_2 was not observed in the deep layers of the skin, or underneath the SC. We were not able to detect TiO_2 below the SC even in the proximity of follicles. Nevertheless, Ti was clearly detected on the uppermost part of the skin samples contacted with naked AR nano-TiO_2 in DMSO aqueous medium. This implies that a significant amount of naked AR nano-TiO_2 strongly adheres to the SC and it was not removed by the washing procedure. On the contrary, the X-ray fluorescent emission of Ti was not detect throughout the whole skin portion contacted with silane– (AR-SL) and silane–silica– (AR-SL-S) coated nano-TiO_2. This demonstrates that coated nano-TiO_2 samples were efficiently removed by the washing procedure performed on the skin after the drug permeation experiment. Such findings are consistent with the results of a previous study recently conducted by some of us (Turci et al., 2013) on a set of naked nano-TiO_2 bearing different surface net charges. They further support that surface charge and not other physico-chemical parameters, including particle lipophilic properties, is the key parameter in driving nano-TiO_2 adhesion to skin.

3.4 Spectroscopic investigation of the stretching mode of lipids and proteins in the SC

Raman spectroscopy has been successfully used to detect spectral changes in malignant and pre-malignant cells (Lyng et al., 2007), to elucidate the conformational alterations induced by solvent on the secondary structure of keratin in isolated corneocytes (Zhang et al., 2007), and to investigate the SC in psoriatic skin (Osada et al., 2004; Bernard et al., 2007) and in general is a well-assessed and valuable tool for investigating in vitro and in vivo cells and tissues (Ali et al., 2013). In this study, the conformational changes induced on lipids and proteins of the SC by TiO_2 have been followed investigating the symmetric and asymmetric vibrational stretching modes of CH, CH_2 and CH_3. By using a confocal Raman microscope, the laser beam has been focused on a few microns wide portion of the SC, delivering a power of ca. 15 mW on the sample. The spectra collected from at least 10 independent analysis of SC contacted with AR, AR-SL and AR-SL-S in DMSO aqueous medium are reported in Figure 3 and compared to the untreated skin. All spectra were baseline subtracted, averaged, and normalized setting the maximum at 2937 cm^{-1} to 1 Raman intensity arbitrary unit. The band assignment is reported following the literature (Anigbogu et al., 1995): $\nu_s(CH_2)$ at 2852 cm^{-1}, $\nu_a(CH_2)$ at 2883 cm^{-1}, $\nu_s(CH_3)$ at 2937 cm^{-1}, $\nu_a(CH_3)$ at 2974 cm^{-1}, and ν(CH) olefinic at 3060 cm^{-1}. The various modes can also be ascribed to proteins and lipids respectively according the work of Anigbogu et al. (1995) being the $\nu_s(CH_2)$, and $\nu_a(CH_2)$ mostly due to lipids and $\nu_s(CH_3)$, $\nu_a(CH_3)$, and ν(CH) olefinic predominantly associated to proteins. The spectra reported show some differences in the CH_2 region, relevant to lipids. In particular, the spectra of SC contacted with coated TiO_2, AR-SL and AR-SL-S, are almost superimposable with the spectrum of uncontacted skin (spectra *b*, *c*, and *a*, respectively), while a relative increase of the intensity of the CH_2 stretching modes (both symmetric and asymmetric) is clearly observed for the sample contacted with AR (spectrum *d*). This could be consistent with a partial structural rearranging of the lipidic chains (Tfayli et al., 2012). In fact, in lipids, the ratio of the symmetric methylene C–H stretching-mode intensities (peak height I_{2890}/I_{2850}) is sensitive to the packing order of the acyl chains and the observed relative increase of intensity of the 2850 cm^{-1} band with respect to 2890 cm^{-1} may account for a change of the lipids bilayer structure (Vyumvuhore et al., 2013). This

phenomenon, occurring with naked AR, but not with coated TiO_2 with similar titania core, is possibly due to physical interaction of nano-TiO_2 with the SC lipids and/or to some TiO_2-induced chemical oxidative damage (Gaber and Peticolas, 1977; Gniadecka et al., 1998 and Wegener et al., 1996).

3.5 Transition enthalpies of lipids in the SC.

The interaction between nano-TiO_2 and SC lipids were investigated by DSC. In this study the lamellar-disordered structure thermal transition at 70 °C, relative to the lipids of the porcine skin SC, was evaluated after treatment with TiO_2 (5 mg/ml) in 10% DMSO aqueous medium. Aqueous suspensions of amorphous silica nanoparticles (5 mg/ml) and hydrogen peroxide solution (0.01 wt. %) were used as negative and positive control, respectively. The decrease in enthalpy values of the skin lipid transition in the presence of naked, compared to transition enthalpy of untreated skin, may indicate that this TiO_2 sample perturbs the intercellular lipid packing arrangement of the SC (Figure 4). However, DSC data indicate that silane and silane-silica coated nano-TiO_2 does not induce a perturbation of the lipid bilayer structure. The result correlates with the structural alteration of the SC measured by Raman spectroscopy.

3.6 Generation of carbon-centered radical and cell-free lipoperoxidation assay

To quantify the capability of nano-TiO_2 to generate a carboxyl radical ($\bullet CO_2^-$) from a stable organic precursor (formate anion, HCO_2^-), the three suspensions were placed in contact with a buffered solution of sodium formate in the presence of DMPO as spin trapping agent. Formate ion is a convenient and largely employed model for the C–H bond occurring in bio-molecules such as peptides, proteins and lipids. The induced rupture of the C–H in formate, thus the capability of a nanoparticles to abstract a hydrogen atom from the formate ion (HCO_2^-), yields to the formation of a carbon-centered carboxyl radical ($\bullet CO_2^-$). Such radical can be detected via the spin trapping technique and EPR spectroscopy, provided that concentrated HCO_2^- and neutral buffered solutions

are employed. Since AR, AR-SL, and AR-SL-S are characterized by the same crystalline phases (90% anatase, 10% rutile), but differ for the presence or for the nature of the coating materials, their reactivity towards formate ion may be employed as an index of the coating efficiency in preventing the dust reactivity possibly implied in the toxic mechanism.

The result of the generation of carbon-centered radical and cell-free lipoperoxidation assay are reported in figure 5. EPR spectra recorded after 60 minutes of incubation of formate ion with the same amounts of AR, AR-SL, and AR-SL-S are reported in figure 5A. A rather intense $\bullet CO_2^-$ signal was detected with the AR sample. A weak signal due to $\bullet CO_2^-$ (superimposed to another signal, possibly due to the generation of an oxygen-centered radical) was detected with AR-SL evidencing that the coating of AR-SL particles is not able to completely inhibit the reactivity of this sample. This may be due to the incomplete coating of the AR-SL particles that may cause the partial exposure of the TiO_2 naked surface allowing it to react with the formate ion. No signal was detected with AR-SL-S indicating that the coating efficiently prevents the onset of $\bullet CO_2^-$ release. The experiment was carried out in the same conditions without the nano-TiO_2 (blank) and no EPR signal was detected.

The potential of nano-TiO_2 to induce lipid peroxidation was assessed by means of thiobarbituric acid (TBA) assay using linoleic acid as a target. To take into account the autoxidative processes that may induce the peroxidation of linoleic acid in the presence of O_2, the same experiment was carried out on a blank dispersion of linoleic acid in the absence of TiO_2. In figure 5B, the amount of MDA detected in solution after 72 hours of incubation of linoleic acid with nano-TiO_2 is reported. AR and AR-SL are rather active in inducing lipid peroxidation. A correlation between the reactivity towards linoleic acid and formate is commonly observed. The peroxidation of linoleic acid by AR in fact correlates with the reactivity towards formate ion reported above (Figure 5A). The strong peroxidation induced by AR-SL is however accompanied by a low reactivity towards formate. This apparent discrepancy is explained by the hydrophobic coating of AR-SL which determines a more

efficient interaction of the lipophilic molecules of linoleic acid with AR-SL surface and consequently a low radical yield possibly drives the strong lipoperoxidation observed.

[INSERT HERE FIGURE 5]

4. Discussion

AmB is a drug of choice for systemic fungal infections and is here used as model molecule for the drug permeation study. AmB bulky structure prevents the drug to diffuse through the skin (Dollery et al., 1991; Manosroi et al., 2004). The low diffusion coefficient of AmB allows to detect small differences of AmB permeation through the skin and to study the potential enhancing effects of chemicals and nanomaterials. In this work, the influence of naked or coated nano-TiO_2 on AmB flux through pig skin was evaluated ex vivo. As a consequence of the changed physico-chemical features, the biological activity of the coated nano-TiO_2 surface is expected to be dramatically different from that of the naked TiO_2. In fact the most significant differences in skin permeation observed in this study are related to the different coatings of nano-TiO_2, while different dispersion media show little influence on the efficiency of drug permeation. A strong increase in the drug flux (Figure 1A) was observed for the skin contacted with naked AR, while no effect was induced by the two coated nano-TiO_2 (AR-SL and AR-SL-S). The experiments were carried out both in an O/W emulsion and in a simplified DMSO aqueous medium. Similar results were obtained in all cases and DMSO aqueous medium was used to further investigate the nano-TiO_2 interaction with skin. To gain a mechanistic insight of the enhancing effect induced by naked TiO_2, a comparative evaluation of the interaction of nano-TiO_2 with skin, and specifically with stratum corneum, was developed. Due to its positive surface charge, only naked AR was found to irreversibly adhere to the negatively charged corneocytes of the SC (micro-XRF). Negatively charged AR-SL and AR-SL-S were both easily removed by washing, but differentiation in term of surface reactivity was observed. The imperfect coating (Carlotti et al., 2009) and the lipophilic nature of AR-SL could explain the high rate of lipid peroxidation measured in the cell-free test. However, despite this significant chemical reactivity, AR-SL, when contacted with skin, did not induce structural alterations of the lipids in the stratum corneum (Raman spectroscopy), nor yielded an enhancement in drug permeation. Table 2 correlates the effects (adhesion and oxidative potential) of the nano-TiO_2 surface characteristics (charge and coating) with the outcomes on skin permeation. Both a strong electrostatically-driven

adhesion between nano-TiO_2 and the skin, and a significant oxidative potential are simultaneously required to decrease the intermolecular order of lipids and alter the intercellular lipid packing arrangement in the SC, which in turn determines the increase of skin permeability (William and Barry, 2004).

The net surface charge and the oxidative potential are hence the two key physico-chemical properties of nano-TiO_2 governing the oxide interaction with the skin. It is worth noting that our data were obtained under controlled light illumination with a very low UV content (< 1 mW/m^2) where the strong photochemical activity of TiO_2 is not activated and correctly simulate an indoor scenario. Reasonably, full sunlight (average UV irradiance > 50 W/m^2) could further enhance the skin permeability. The synergic effect of UV irradiation and TiO_2 photo-activity on skin permeability is still an intriguing and debated subject (Jatana and DeLouise, 2014) and should be the subject for future investigation.

5. Conclusion

Our findings suggest that increased permeability of the SC induced by nano-TiO_2 may be intentionally used to enhance the permeation of chemicals, such as drugs, through the skin, favoring the transdermal drug delivery. Naked nano-TiO_2, delivered both in a simplified DMSO aqueous medium and in more realistic O/W emulsion, enhanced the drug flux through the skin. Nano-TiO_2 enhancing effect may be easily tuned by modifying particle net surface charge (e.g., varying the anatase/rutile ratio (Ruan et al., 2013)) and its chemical potential precisely assessed by in vitro inexpensive tests. On the contrary, the enhancer effect of naked nano-TiO_2 must be carefully evaluated when the transdermal translocation of bioactive molecules ought to be avoided, as in the case of cosmetic products and sunscreen lotions.

Funding

Financial support from Regione Piemonte (project CIPE NANOSAFE) is gratefully acknowledged.

Acknowledgments

Micro-Raman spectra and fiber image analysis have been obtained with the equipment acquired by the Interdepartmental Center “G. Scansetti” for Studies on Asbestos and Other Toxic Particulates with a grant from Compagnia di San Paolo, Torino, Italy.

References

Al-Saidan, S.M., Barry, B.W., Williams, A.C., 1998. Differential scanning calorimetry of human and animal stratum corneum membranes. Int. J. Pharm. 168, 17-22.

Ali, S.M., Bonnier, F., Lambkin, H., Flynn, K., McDonagh, V., Healy, C., Lee, T.C., Lyng, F.M., Byrne, H.J., 2013. A comparison of Raman, FTIR and ATR-FTIR micro spectroscopy for imaging human skin tissue sections. Anal. Methods 5, 2281-2291.

Anigbogu, A. N. C., Williams, A. C., Barry, B. W., Edwards, H. G. M., 1995. Fourier-transform Raman-spectroscopy of interactions between the penetration enhancer dimethyl-sulfoxide and human stratum-corneum. Int. J. Pharm. 125, 265−282.

Baroli, B., 2010. Penetration of nanoparticles and nanomaterials in the skin: Fiction or reality? J. Pharm. Sci. 99, 21−50.

Bennat, C., Mueller-Goymann, C.C., 2000. Skin penetration and stabilization of formulations containing microfine titanium dioxide as physical UV filter. Int. J. Cosmetic Sci. 22, 271-283.

Bernard, G., Auger, M., Soucy, J., Pouliot, R., 2007. Physical characterization of the stratum corneum of an in vitro psoriatic skin model by ATR-FTIR and Raman spectroscopies. Biochim. Biophys. Acta 1770, 1317−1323.

Bolis, V., Busco, C., Ciarletta, M., Distasi, C., Erriquez, J., Fenoglio, I., Livraghi, S., Morel, S., 2012. Hydrophilic/hydrophobic features of TiO_2 nanoparticles as a function of crystal phase, surface area and coating, in relation to their potential toxicity in peripheral nervous system. J. Colloid Interf. Sci. 369, 28-39.

Borm, P.J., Robbins, D., Haubold, S., Kuhlbusch, T., Fissan, H., Donadson, K., Schins, R., Stone, V., Kreyling, W., Lademann, J., Krutmann, J., Warheit, D., and Oberdorster, E., 2006. The potential risks of nanomaterials: a review carried out for ECETOC. Part. Fibre Toxicol. 3, 11.

Carlotti, M. E., Sapino, S., Vione, D., Minero, C., Peira, E., Trotta, M., 2007. Study on the photodegradation of salicylic in the absence and in the presence of TiO2. J. Disper. Sci. Technol. 28, 805−818.

Carlotti, M. E., Ugazio, E., Sapino, S., Fenoglio, I., Greco, G., and Fubini, B., 2009. Role of particle coating in controlling skin damage photoinduced by titania nanoparticles. Free Radical Res. 43, 312−322.

Daimon, T., Hirakawa, T., Kitazawa, M., Suetake, J., Nosaka, Y., 2008. Formation of singlet molecular oxygen associated with the formation of superoxide radicals in aqueous suspensions of TiO_2 photocatalysts. Appl. Catal., A. 340, 169-175.

Diebold, U., 2003. The surface science of titanium dioxide. Surf. Sci. Rep. 48, 53-229.

Dollery, C., 1991. Therapeutic Drugs. Churchill Livingstone, New York.

Dussert, A.-S., Gooris, E., Hemmerle., J., 1997. Characterization of the mineral content of a physical sunscreen emulsion and its distribution onto human stratum corneum. Int. J. Cosmetic Sci. 19, 119–129.

Elias, P. M., 2005. Stratum corneum defensive functions: an integrated view. J. Invest. Dermatol. 125, 183-200

Fenoglio, I., Fubini, B., Ghibaudi, E. M., Turci, F., 2011. Multiple aspects of the interaction of biomacromolecules with inorganic surfaces. Adv. Drug Deliver. Rev. 63, 1186−1209.

Fenoglio, I., Ponti, J., Alloa, E., Ghiazza, M., Corazzari, I., Capomaccio, R., Rembges, D., Oliaro-Bosso, S., Rossi, F., 2013. Singlet oxygen plays a key role in the toxicity and DNA damage caused by nanometric TiO2 in human keratinocytes. Nanoscale 5, 6567−6576.

Franz, T. J. Percutaneous absorption. On the relevance of in vitro data. J. Invest. Dermatol. 1975, 64, 190–195.

Gaber, B. P., and Peticolas, W. L., 1977. On the quantitative interpretation of biomembrane structure by Raman spectroscopy. Biochim. Biophys. Acta 465, 260−274.

Gamer, A.O., Leibold, E., van Ravenzwaay, B., 2006. The in vitro absorption of microfine zinc oxide and titanium dioxide through porcine skin. Toxicol. in Vitro 20, 301–307.

Gniadecka, M., Nielsen, O. F., Christensen, D. H., and Wulf, H. C., 1998. Structure of water, proteins, and lipids in intact human skin, hair, and nail. J. Invest. Dermatol. 110, 393−398.

Jatana, S., DeLouise, L. A., 2014. Understanding engineered nanomaterial skin interactions and the modulatory effects of ultraviolet radiation skin exposure. WIREs Nanomed Nanobiotechnol, 6, 61–79. doi: 10.1002/wnan.1244

Lee, S. H., Jeong, S. K., Ahn, S. K., 2006. An update of the defensive barrier function of skin. Yonsei. Med. J. 47, 293-306.

Lyng, F. M., Faolain, E. O., Conroy, J., Meade, A. D., Knief, P., Duffy, B., Hunter, M. B., Byrne, J. M., Kelehan, P., and Byrne, H. J., 2007. Vibrational spectroscopy for cervical cancer pathology, from biochemical analysis to diagnostic tool. Exp. Mol. Pathol. 82, 121−129.

Manosroi, A., Kongkaneramit, L., Manosroi, J., 2004. Stability and transdermal absorption of topical amphotericin B liposome formulations. Int. J. Pharm. 270, 279-286.

Menzel, F., Reinert, T., Vogt, J., Butz, T., 2004. Investigation of percutaneous uptake of ultrafine TiO_2 particles at the high energy ion nanoprobe LIPSION. Nucl. Instr. And Meth. In Phys. Res. B. 219-220, 82-86.

Mitsui, T., 1997. New Cosmetic Science. Elsevier Science B.V., Amsterdam, The Nederlands.

Newman, M.D., Stotland, M., Ellis, J.I., 2009. The safety of nanosized particles in titanium dioxide and zinc oxide-based sunscreens. J. Am. Acad. Dermatol. 61, 685-692.

Osada, M., Gniadecka, M., and Wulf, H. C., 2004. Near infrared Fourier transform Raman spectroscopic analysis of proteins, water and lipids in intact normal stratum corneum and psoriasis scales. Exp. Dermatol. 13, 391−395.

Padula, C., Nicoli, S., Santi, P., 2011. In vitro evaluation of bioadhesive films containing ibuprofen. Anti-Inflammatory and Anti-Allergy Agents in Medicinal Chemistry 10, 240-245.

Pflücker, F., Wendel, V., Hohenberg, H., Gartner, E., Will, T., Pfeiver, S., Wepf, R., Gers-Barlag, H., 2001. The human stratum corneum layer: an effective barrier against dermal uptake of different forms of topically applied micronised titanium dioxide. Skin Pharmacol. Appl. Skin Physiol. 14 (Suppl. 1), 92–97.

Ruan, P., Qian, J., Xu, Y., Xie, H., Shao C., Zhou X., 2013. Mixed-phase TiO_2 nanorods assembled microsphere: crystal phase control and photovoltaic application. Cryst. Eng. Comm. 15, 5093-5099

Schulz, J., Hohenberg, H., PXucker, F., Gartner, E., Will, T., PfeiVer, S., Wepf, R., Wendel, V., Gers-Barlag, H., Wittern, K.P., 2002. Distribution of sunscreens on skin. Adv. Drug Deliver. Rev. 54, S157–S163.

Serpone, N., Dondi, D., and Albini, A., 2007. Inorganic and organic UV filters: their role and efficacy in sunscreens and suncare product. Inorg. Chim. Acta 360, 794−802.

Silva, C. G., Faria, J. L., 2009. Anatase vs. rutile efficiency on the photocatalytic degradation of clofibric acid under near UV to visible irradiation. Photochem. Photobiol. Sci. 8, 705-711.

Tfayli, A., Guillard, E., Manfait, M., Baillet-Guffroy, A., 2012. Molecular interactions of penetration enhancers within ceramides organization: a Raman spectroscopy approach. Analyst 137, 5002-5010.

Turci, F., Peira, E., Corazzari, I., Fenoglio, I., Trotta, M., Fubini, B., 2013. Crystalline phase modulates the potency of nanometric TiO_2 to adhere to and perturb the stratum corneum of porcine skin under indoor light. Chem. Res. Toxicol. 26, 1579−1590.

Vyumvuhore, R., Tfayli, A., Duplan, H., Delalleau, A., Manfait, M., Baillet-Guffroy, A., 2013. Raman spectroscopy: a tool for biomechanical characterization of Stratum Corneum. J. Raman Spectrosc. 44, 1077–1083. doi: 10.1002/jrs.4334.

Wegener, M., Neubert, R., Rettig, W., and Wartewig, S., 1996. Structure of stratum corneum lipids characterized by FT-Raman spectroscopy and DSC. 1. Ceramides. Int. J. Pharm. 128, 203−213.

Wilkinson, J.M., McDonald, C., Parkin, J.E., Sunderland, V.B, 1998. A high-performance liquid-chromatographic assay for amphotericin B in a hydrophilic colloidal paste base. J. Pharm. Biomed. Anal. 17, 751-755.

Williams AC, Barry BW., 2004. Penetration enhancers. Adv. Drug Deliver. Rev. 56(5), 603-18.

Yamane, M. A., Williams, A. C., Barry, B. W., 1995. Effects of terpenes and oleic-acid as skin penetration enhancers towards 5- fluorouracil as assessed with time; permeation, partitioning and differential scanning calorimetry. Int. J. Pharm. 116, 237−251.

Zhang, G. J., Moore, D. J., Flach, C. R., and Mendelsohn, R., 2007. Vibrational microscopy and imaging of skin: From single cells to intact tissue. Anal. Bioanal. Chem. 387, 1591−1599.

TABLE CAPTIONS

Table 1. Physico-chemical characteristics of nano-TiO2 samples. Crystal phase composition, particle size, surface area, surface coating, mean hydrodynamic diameter (dH), polydispersity index (PDI), and ζ potential of nano-TiO2 agglomerates/aggregates in the DMSO aqueous medium are specified.

Table 2. Summary of the effects of nano-TiO2 surface characteristics on the outcomes on the SC structure and the AmB permeation through the skin.

Table 1

Commercial name	**Sample name**	**Crystal phase composition** [1]	**Primary particle size**[1] **(nm)**	**Surface area**[2] **(m^2/g)**	**Coating** [3]	**pH suspension**	**d_H (nm) ± S.E.** [4]	**PDI**[4]	**ζ potential ± S.E.** [5]
Aeroxide P25	AR	anatase/rutile 9:1	30±4 (A) 50±6 (R)	53	-	5.40	266.0 ± 10.4	0.129	+9.10 mV ± 0.17
PW Covasil S-1	AR-SL	anatase/rutile 9:1	26±1 (A) 44±8 (R)	43	TMCS < 5%	6.00	190.0 ± 4.0	0.324	−17.1 mV ± 0.51
Tego Sun TS plus	AR-SL-S	anatase/rutile 9:1	19±4 (A) 34±3 (R)	60	SiO_2 10-25% TMCS < 4.5%	6.02	207.8 ± 12.6	0.329	−20.7 mV ± 0.50

[1] Evaluated by Rietveld refinement of XRPD data (Bolis et al., 2012) and Raman spectroscopy (Figure S1)
[2] Evaluated by means of N_2-BET technique
[3] As declared by the producer
[4] Evaluated by means of dynamic light scattering (DLS)
[5] Evaluated by means of electrophoretic light scattering [ELS]

Table 2

	nano-TiO_2 physical interaction with skin	**in vitro oxidative potential**		**outcomes on skin**	
	adhesion to SC [1]	*C–H radical rupture [2]*	*lipid peroxidation [3]*	*SC structural alteration [4]*	*Enhanced drug flux [5]*
AR	+	+	+	+	+
AR-SL	–	+/–	+	–	–
AR-SL-S	–	–	–	–	–

Evaluated by means of: [1] μ-XRF on skin sections; [2] spin-trapping/EPR spectroscopy with formate ion as target molecule; [3] in vitro MDA assay with linoleic acid; [4] micro-Raman spectroscopy on skin thin sections and DSC of detached SC; [5] drug content variation in the receiving phase, HPLC.

FIGURE CAPTIONS

Figure 1. Variation of flux through (A) and accumulation (B) in skin of AmB, induced by the occurrence of naked anatase/rutile (AR), silane-coated (AR-SL) and silane-silica coated (AR-SL-S) nano-TiO2 samples, with respect to skin not brought in contact with TiO2. Experiments were performed dissolving the drug in two media with different hydrophilicity: 10% DMSO aqueous solution (light gray bars) and oil/water emulsion (dark gray).

Figure 2. Chemiometric mapping of nano-TiO2 in the skin. The μ-XRF elemental chemiometric mapping of skin thin cross sections (imaged at 100×, a) for Si, Cl and Ti (b, c, and d respectively) is reported as pseudocolor image with a resolution of 32×25 pixel. Untreated (A) and AR-contacted (B) skin were analyzed. Normalized ROI intensity of Kα fluorescent lines was reported adopting a monochromatic scale. The SC is highlighted with a dotted line, and lines are drawn in chemiometric panels to help reader's eyes.

Figure 3. Raman spectra of the CH stretching band of lipid and proteins in the SC. Thin cross sections were analyzed focusing the laser beam on an intact portion of the SC. The Raman spectra from untreated (negative control, spectrum a) and TiO2–contacted skin (AR-SL, AR-SL-S, and AR, spectra b, c, and d, respectively) are reported. At least 10 independent spectra were recorded, baseline subtracted, averaged, and normalized setting the maximum intensity to 1 arbitrary unit (A.U.).

Figure 4. Variation of the lipid transition enthalpies in the stratum corneum of nano-TiO2 contacted skin. The lipid transition enthalpy normalized by the transition enthalpy of untreated skin (ΔH%) was compared to a positive (Ctrl+) and a negative (Ctrl -) control (hydrogen peroxide and amorphous nano-SiO2 respectively). Data are reported as mean ± SD of at least three independent measures.

Figure 5. Generation of carbon-centered radicals and in vitro lipoperoxidation under indoor illumination. (A) EPR spectra recorded on the suspension of AR, AR-SL, and AR-SL-S nano-TiO2 in a solution of 1 M of sodium formate and 0.085 M DMPO in 0.25 M phosphate buffer, pH 7.4, after 1 incubation under indoor illumination. The EPR spectrum recorded in the same condition but in the absence of nano-TiO2 (blank) is also reported. (B) By means of thiobarbituric acid (TBA) assay, MDA was measured on the supernatant after incubation of AR, AR-SL and AR-SL-S nano-TiO2 suspended in a 1 mM dispersion of linoleic acid in 5 mM phosphate buffer (pH 7.4) for 72 h under indoor illumination. A linoleic acid dispersion without dust was employed as blank. The data are expressed as the mean value of three separate determinations ± SD.

Figure 1 (A)

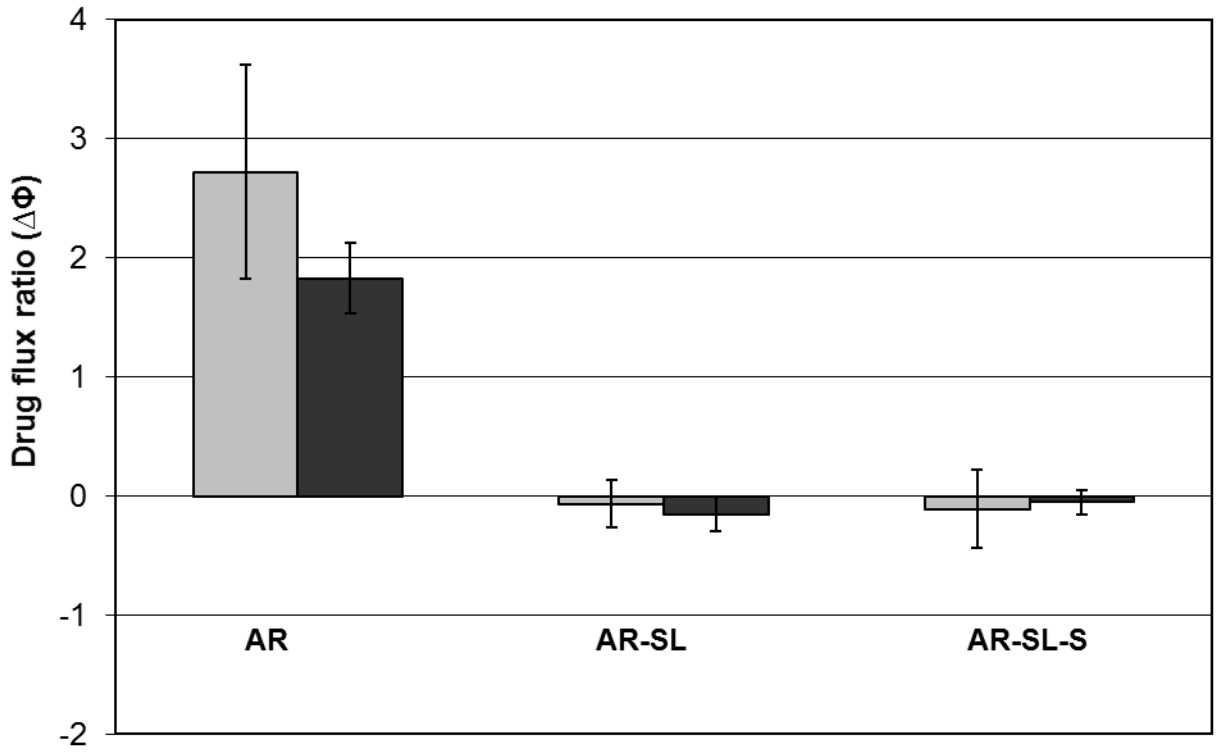

Figure 1 (B)

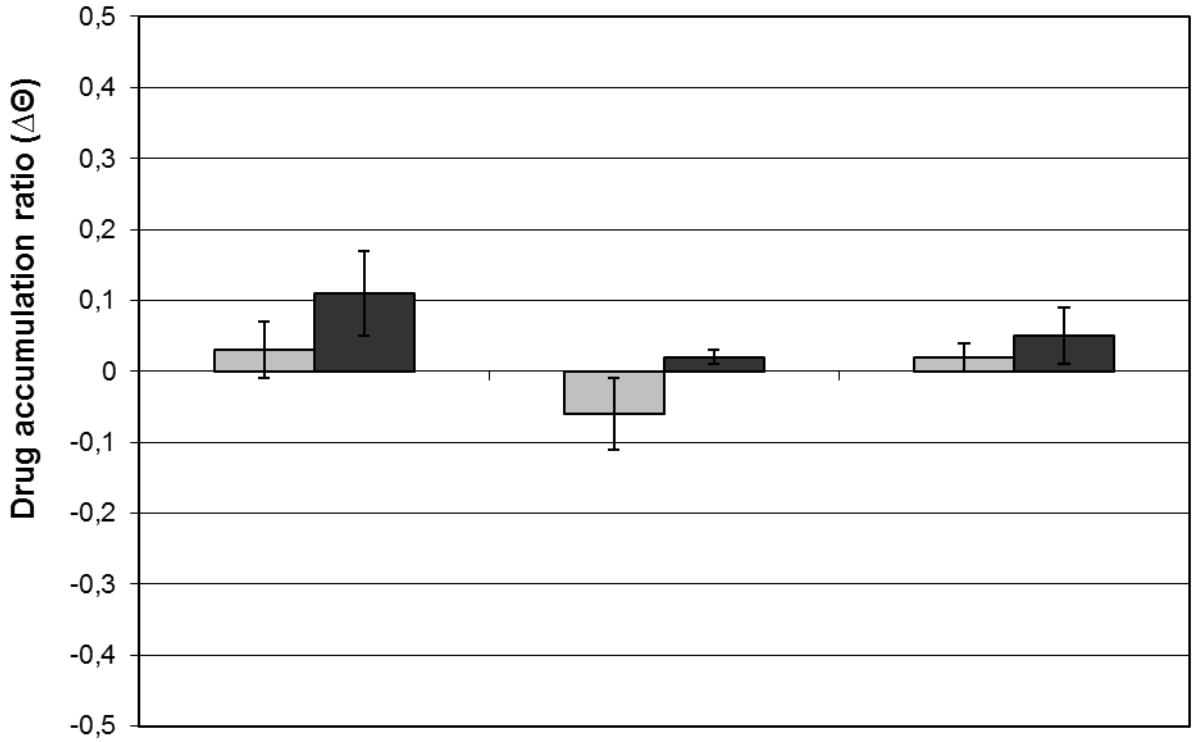

Figure 2

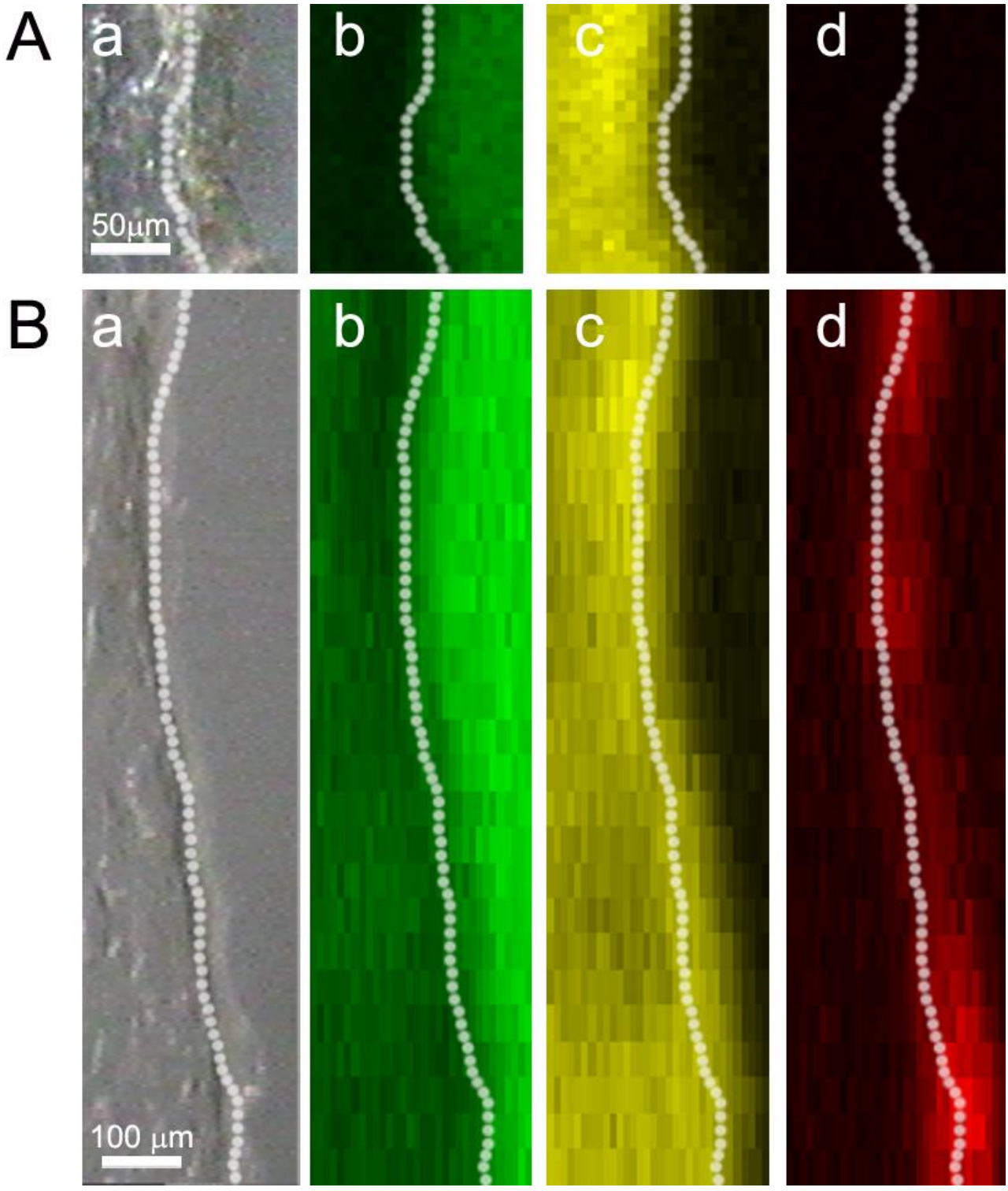

Figure 3

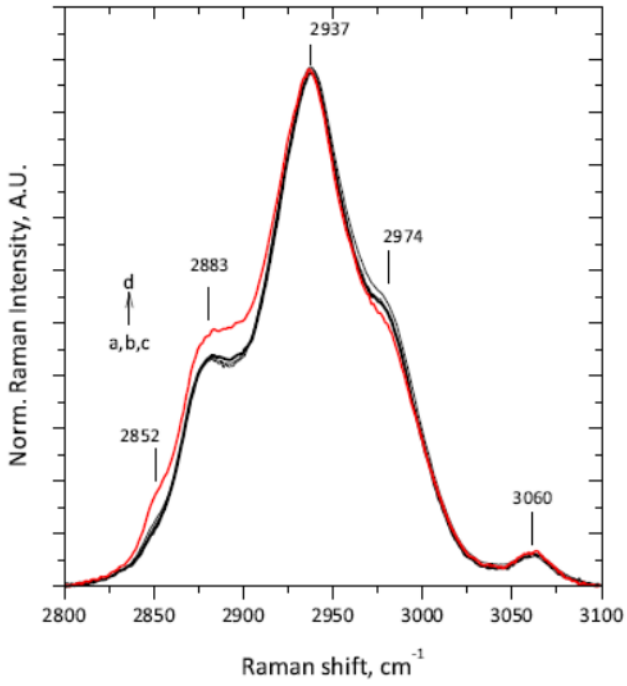
2937
2974
2883
d
a,b,c
2852
3060
Norm. Raman Intensity, A.U.
2800
2850
2900
2950
3000
3050
3100
Raman shift, cm-1

Figura 4

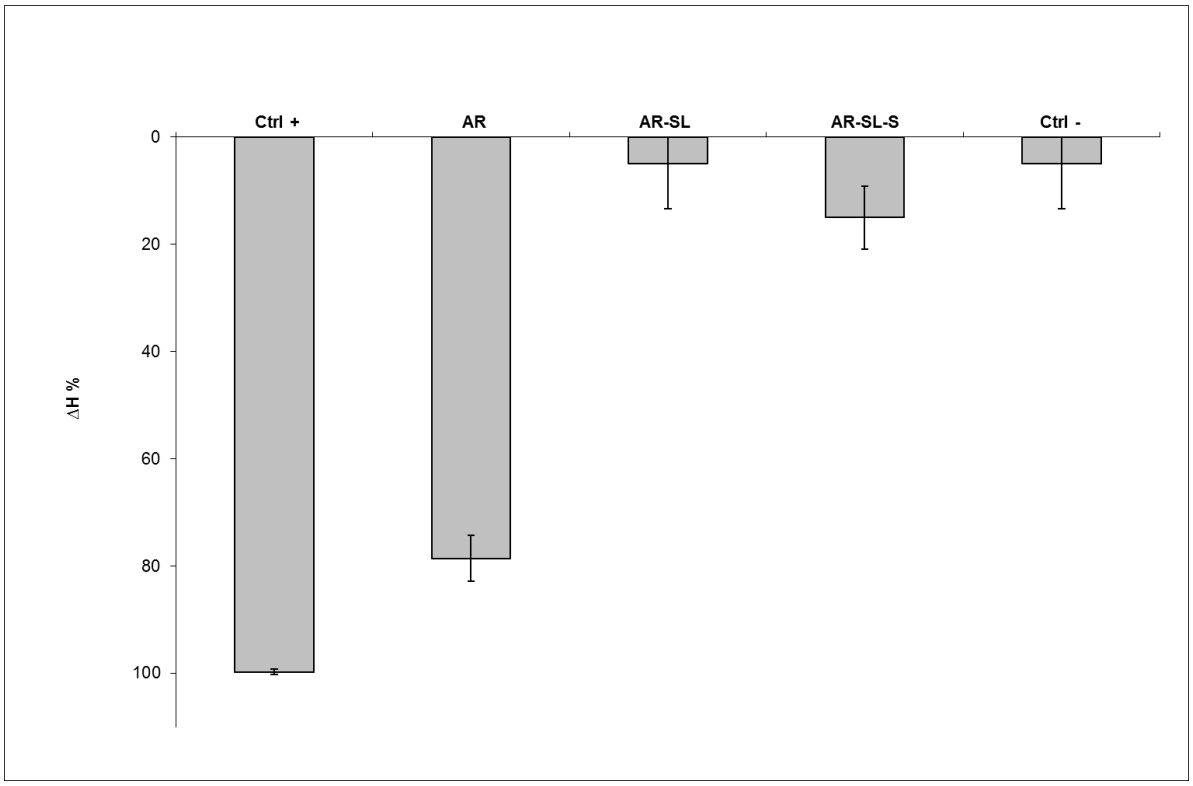

Figure 5

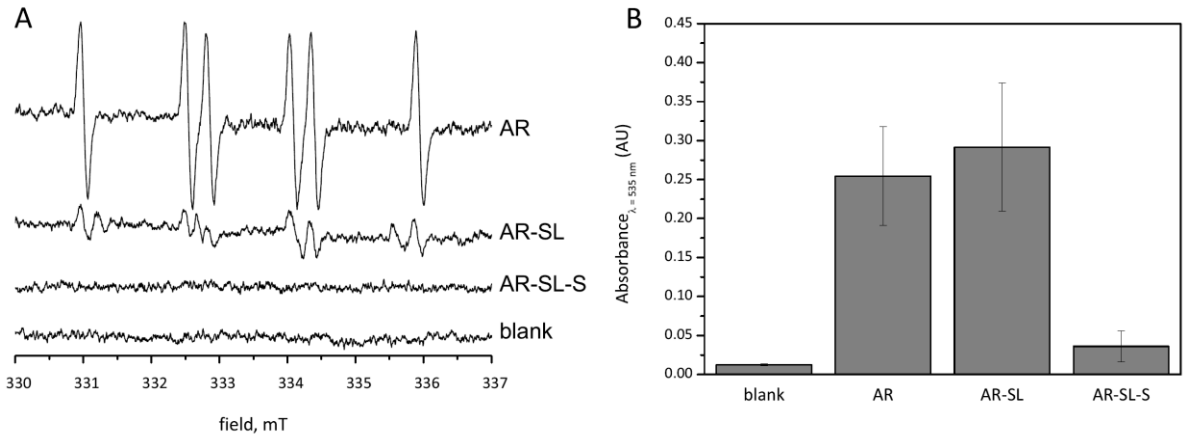
A
AR
AR-SL
AR-SL-S
blank
330
331
332
333
334
335
336
337
field, mT
B
Absorbance λ = 535 nm (AU)
0.45
0.40
0.35
0.30
0.25
0.20
0.15
0.10
0.05
0.00
blank
AR
AR-SL
AR-SL-S